SIMULATION OF MACROSEGREGATION IN THE DC CASTING OF BINARY ALUMINUM ALLOYS

SIMULACIJA MAKROIZCEJANJA PRI POLKONTINUIRNEM ULIVANJU BINARNIH ALUMINIJEVIH ZLITIN

Miha Založnik[1], Božidar Šarler[2], Dominique Gobin[3]

[1]Impol, d. d., Sektor razvoj, Partizanska 38, 2310 Slovenska Bistrica, Slovenija
[2]Politehnika Nova Gorica, Laboratorij za večfazne procese, Vipavska 13, 5000 Nova Gorica, Slovenija
[3]Laboratoire FAST, UMR CNRS 7608, Campus Universitaire, Bât. 502, 91405 Orsay cedex, France
miha.zaloznik@p-ng.si

A common defect that occurs in direct-chill (DC) casting is macrosegregation: an inhomogeneous distribution of alloy components across the cross-section of the solidified casting. This defect can lead to non-uniform mechanical properties, which affect the behavior of the metal during downstream forming and heat treatments. The main mechanism behind macrosegregation is the transport of segregated alloying elements at the scale of the casting by the relative movement of liquid and equiaxed solid grains in the mushy zone, induced as well by pouring as by thermal and solutal natural convection. These macroscopic phenomena are physically quite well understood, yet very difficult to quantitatively model. In this work, first results obtained from an axisymmetric computational model of the DC casting of aluminum alloy billets are presented. The physical model of the solute transport is based on the one-phase continuum mixture model of dendritic solidification, supplemented by constitutive models of microsegregation. It takes into account solute transport by diffusion and advection. A rigid solid phase is assumed. The coupled mass, momentum, energy and solute conservation equations and microsegregation models are solved using the finite-volume method (FVM). The results of simulations of macrosegregation in an Al-4,5 % mass fraction of Cu billet are presented and explained. The model's deficiencies related to numerical discretization errors and physical modeling are recognized and identified as issues for further research.

Keywords: solidification; direct-chill casting; macrosegregation; modeling

Makroizcejanje, neenakomerna porazdelitev legirnih elementov po ulitku je pogost defekt pri polkontinuirnem ulivanju. Povzroči lahko neenakomerne mehanske lastnosti materiala, ki poslabšajo njegove karakteristike med nadaljnjimi postopki obdelave. Makroizcejanje je posledica transporta legirnih elementov na merilu ulitka zaradi relativnega gibanja kapljevinaste faze in enakoosnih kristalnih zrn v trdno kapljevinastem medfaznem območju. Do gibanja faz pride zaradi naravne konvekcije zaradi temperaturnih in koncentracijskih gradientov ter zaradi prisilnega toka pri vtoku taline. Poznanje posameznih makroskopskih pojavov je pri tem dokaj dobro, vendar jih je zelo težko kvantitativno modelirati. V tem delu so predstavljeni prvi rezultati numeričnega modela makroizcejanja pri polkontinuirnem ulivanju. Fizikalni model transporta sestavin temelji na kontinuumskem modelu enofazne mešanice za dendritsko strjevanje. Dopolnjujejo ga konstitutivni modeli za opis mikroizcejanja. Model upošteva transport sestavin z difuzijo in advekcijo zaradi toka kapljevine, pri čemer je v kašastem medfaznem območju predpostavljena toga trdna faza. Sklopljene enačbe ohranitve mase, gibalne količine, energije in sestavin ter mikroizcejni modeli se rešujejo z metodo kontrolnih prostornin. Predstavljeni in pojasnjeni so rezultati simulacij makroizcejanja v drogu iz binarne zlitine Al-4,5 % Cu. Ugotovljene so nekatere pomanjkljivosti modela zaradi numeričnih diskretizacijskih napak in nepopolnosti fizikalnega modela. Ti področji sta razpoznani kot relevantni področji za nadaljnje raziskave.

Ključne besede: strjevanje; polkontinuirno ulivanje; makroizcejanje; modeliranje

1 INTRODUCTION

Solidification is one of the key phenomena in the processing of metals. Most metals used for technical applications are alloys, i.e., mixtures composed of several chemical components. The solidification of such mixtures differs in many respects from that of pure substances. Phase change takes place over a range of temperatures, thus solid and liquid can coexist in equilibrium at various temperatures. Moreover, due to different solubilities in the solid and liquid phases the components can be rejected from or preferentially included into the forming phase (segregation). The solid-liquid interface is usually not smooth and develops into a complex microscopic growth structure, macroscopically regarded as a mixture zone of coexisting solid and liquid phases, called the mushy zone. The processes of heat, mass and species transfer in the mushy zone are closely interlinked.

One of the most widely used industrial metal processing technologies is direct-chill (DC) casting. During casting many defects can occur that are a direct consequence of the transport phenomena taking place in the process. A common defect that occurs in the direct-chill casting of aluminum alloys is macrosegregation, an inhomogeneous distribution of alloy components in the solidified casting. It is caused by solute transport, primarily due to the flow of segregated liquid in the mushy zone, which is a result of

- buoyancy forces due to thermal gradients (thermal natural convection),
- buoyancy forces due to concentration gradients (solutal natural convection),

- density differences between the two phases (solidification shrinkage),
- inlet flow (bulk convection).

Macrosegregation can lead to non-uniform mechanical properties that affect the behavior of the metal during subsequent treatments. It is therefore desirable to be able to simulate the casting process in order to predict the influence of casting parameters on the resulting macrosegregation pattern. Besides prediction, modeling is aimed at an improved understanding of the basic mechanisms involved.

A commonly observed solute distribution pattern in a DC cast billet shows a one-dimensional radial concentration distribution. A solute-depleted region is present in the billet center, adjoined by a positive segregation zone spreading into the outward radial direction, an adjacent thin negative segregation zone and another positive segregation layer at the surface. The enriched subsurface layer is attributed to solidification-shrinkage induced flow, while the other patterns are a consequence of an interplay of thermal convection, solutal convection and shrinkage flows. The exact mechanism is not yet completely understood. Recently, the effect of advective species transport by low-concentration free-floating crystal grains has been much discussed as an important factor [1,2,3,4], especially in the formation of the negative centerline segregation zone.

The first numerical-model study of macrosegregation in DC casting was made by Flood, Katgerman and Voller [5]. Their model assumed a rigid mushy zone moving at the casting speed and failed to predict macrosegregation properly. Reddy and Beckermann [6] presented a computational investigation of the influence of grain refining on macrosegregation, where they simulated grain refining via an increased mushy-zone permeability. Good explanations for the computed concentration profiles could not be provided. Generally, models predict positive subsurface segregation, which is attributed to shrinkage flow. Some models also include the effect of exudation on surface macrosegregation, modeled successfully and in detail by Thevik, Mo et al. [7]. A few years ago Vreeman and Incropera [8] revealed a problem pertaining to upwind discretization of the species-transport equation, especially in the simulation of DC casting. They showed that the previously used inconsistent discretization leads to severe errors in the concentration field solution. Subsequent studies thus use the corrected discretization method. Even though the accuracy of the numerical solutions of metal melt flow and species transport during solidification has been addressed in the literature it has mostly been clearly insufficient in simulations of large-scale castings (e.g., in [9]). It thus remains an important issue in further research [10]. Recently, the problem of numerical diffusion in the simulation of macrosegregation in DC casting was addressed by Venneker and Katgerman [11], who performed computations using several finite-volume discretization schemes on different meshes. They did not explicitly consider the flow field; however, they did show that the use of poorly performing discretization schemes induces considerable numerical errors, affecting the predicted macrosegregation profile.

2 DESCRIPTION OF THE MODEL

2.1 Macroscale transport model

The macroscopic conservation equations are transport equations for heat, mass, momentum and species. They are formulated as a one-phase continuum mixture model [12], where the mixture quantities in a two-phase (solid-liquid) mixture are defined in terms of phase quantities and phase fractions as follows.

$$f_i = \frac{m_i}{\sum_j m_j} \quad g_i = \frac{V_i}{\sum_j V_j} \tag{1}$$

$$\rho_m = g_s \rho_s + g_l \rho_l \quad \vec{v}_m = f_s \vec{v}_s + f_l \vec{v}_l$$
$$h_m = f_s h_s + f_l h_l \quad C_m = f_s C_s + f_l C_l \tag{2}$$

Continuity equation for the mixture.

$$\frac{\partial \rho_m}{\partial t} + \nabla \cdot (\rho_m \vec{v}_m) = 0 \tag{3}$$

Mixture momentum conservation equation.

$$\frac{\partial \rho_m \vec{v}_m}{\partial t} + \nabla \cdot (\rho_m \vec{v}_m \vec{v}_m) = -\nabla p + \nabla \cdot \left(\mu_l \frac{\rho_m}{\rho_l} \nabla \vec{v}_m \right)$$
$$- \frac{\mu_l}{K} \frac{\rho_m}{\rho_l} (\vec{v}_m - \vec{v}_s) \tag{4}$$
$$- \rho_l \vec{g} \left[\beta_T (T - T_0) + \beta_C (C_m - C_0) \right]$$
$$- \nabla \cdot \left[\rho_m (f_s \vec{v}_s \vec{v}_s + f_l \vec{v}_l \vec{v}_l - \vec{v}_m \vec{v}_m) \right]$$

The velocity of the solid is defined to be $v_s = v_{cast}$ everywhere, since all the solid mush is assumed to be coalesced in a porous matrix and connected with the bulk solid. The permeability is modeled by the Kozeny-Carman relation $K = K_0 g_l^3 / (1 - g_l)^2$. The mixture energy conservation equation is:

$$\frac{\partial (\rho_m h_m)}{\partial t} + \nabla \cdot (\rho_m \vec{v}_m h_m) = \nabla \cdot (k \nabla T) \tag{5}$$
$$- \nabla \cdot \left[\rho_m (f_s \vec{v}_s h_s + f_l \vec{v}_l h_l - \vec{v}_m h_m) \right]$$

The diffusive term (Fourier law) is reformulated in terms of the mixture enthalpy using the supplementary thermodynamic state equations.

$$h_s(T) = h_{ref} + \int_{T_{ref}}^{T} c_{ps} dT \tag{6}$$

$$h_l(T) = h_s(T) + L_{eut} + \int_{T_{eut}}^{T} (c_{pl} - c_{ps}) dT \tag{7}$$

The final form of the equation is obtained.

$$\frac{\partial(\rho_m h_m)}{\partial t} + \nabla \cdot (\rho_m \vec{v}_m h_m) =$$

$$= \nabla \cdot \left(\frac{k}{c_{ps}} \nabla h_m \right) + \nabla \cdot \left(\frac{k}{c_{ps}} \nabla (h_s - h_m) \right) \qquad (8)$$

$$- \nabla \cdot \left[\rho_m (f_s \vec{v}_s h_s + f_l \vec{v}_l h_l - \vec{v}_m h_m) \right]$$

Mixture species conservation equation.

$$\frac{\partial(\rho_m C_m)}{\partial t} + \nabla \cdot (\rho_m \vec{v}_m C_m) = \nabla \cdot (\rho_m D_m \nabla C_m)$$

$$+ \nabla \cdot \left[\rho_m (f_s D_s \nabla C_s + f_l D_l \nabla C_l - D_m \nabla C_m) \right] \qquad (9)$$

$$- \nabla \cdot \left[\rho_m (f_s \vec{v}_s C_s + f_l \vec{v}_l C_l - \vec{v}_m C_m) \right]$$

The phase quantities (f_s, f_l, h_s, h_l, C_s, C_l) that still appear in the mixture transport equations (3), (4), (8), and (9) are modeled by supplementary thermodynamic models, defining phase enthalpies (Equations (6), (7)) and models of microscale transport phenomena, describing the relations between the local phase concentrations. These models are unified in a so-called microsegregation model, which is described in the following section.

2.2 Microsegregation model

Modeling of the transport of species at the microscale is usually based on the following simplifying assumptions [13].

- One-dimensional model geometry, defined by a control volume between the periodic secondary dendrite arms.
- Perfect mixing in the liquid phase ($C_l = C_l^*$).
- Thermal equilibrium (uniform temperature) at the microscale.
- Thermodynamic equilibrium at the phase interface ($T = T_S(C_l)$, $C_s^* = k_p C_l$).

The microsegregation models are defined by a system of three equations.

1. Definition of mixture enthalpy following from Equations (2), (6), and (7).

$$h_m(T, f_l) = \int_{T_{ref}}^{T} c_{ps} dT + f_l \left[L_{eut} + \int_{T_{eut}}^{T} (c_{pl} - c_{ps}) dT \right] \qquad (10)$$

2. Linearized liquidus line equation.

$$T(C_l) = T_f + m_L C_l \qquad (11)$$

3. Microscale species transport model, which defines the link between the mixture concentration C_m, the liquid concentration C_l and the liquid fraction f_l. In a general form it can be written as

$$C_l(C_m, f_l) \qquad (12)$$

Examples of microscale transport models are the inverse lever rule

$$C_l = \frac{C_m}{k_p + f_l(1 - k_p)} \qquad (13)$$

or the Scheil model (in the differential, open-system formulation)

$$f_l dC_l + (k_p - 1)C_l df_l = dC_m \qquad (14)$$

By the substitution of variables in Equations (10)-(12) it is possible to analytically obtain a function

$$F(f_l) = 0 \qquad (15)$$

The root of the function is found using Newton's method, giving f_l. Then the temperature T can be calculated from Equation (10) and the liquid concentration C_l from Equation (11). The solution of the microsegregation model thus gives the temperature T, the liquid fraction f_l and the liquid concentration C_l from the mixture enthalpy h_m and the concentration C_m, which are obtained from the solution of the macroscopic transport model. The remaining phase quantities needed in the macroscopic model (f_s, h_s, h_l, C_s) are then calculated using Equations (1), (2), (6), and (7).

2.3 Solution procedure

The set of macroscopic transport equations (Equations (3), (4), (8), and (9)) was solved with the finite-volume method (FVM) on an axisymmetric geometrical model. The computer code by Mencinger [14] for the solution of thermal and flow fields in DC casting, which was extended by the macroscopic species transport and microsegregation models, was used. The top boundary at the inflow was assumed to be isothermal at a prescribed casting temperature, the inflow velocity was fixed at $v_{in} = (\rho_s/\rho_l)v_{cast}$. The casting velocity was $v_{cast} = 10^{-3}$ m/s. The bottom boundary was assumed to be adiabatic. Although the latter assumption is not completely valid because of the short domain length, it should not significantly affect the basic mechanisms of macrosegregation. The left boundary (centerline) is adiabatic because of axisymmetry. The slip boundary conditions for velocity and chill boundary conditions describing the heat transfer to the cooling water [11,15] are applied at the right boundary. They are summarized in **Table 1**. **Table 2** summarizes the material properties as already used in [11,15].

The SIMPLE algorithm [16] was used for the pressure-velocity coupling. The upwind-difference scheme was used for the discretization of the advective fluxes in all equations. Because of the high thermal diffusivity of aluminum alloys this is believed to cause only minor numerical diffusion in heat transfer. For momentum and species transport the upwind scheme was used to prevent stability problems with higher order schemes, which would be unstable for the mesh Péclet numbers ($Pe_{\Delta x}$) and mesh Reynolds numbers ($Re_{\Delta x}$) encountered in the advection-diffusion transport of species and momentum respectively.

$$Pe_{\Delta x} = \frac{v \Delta x}{D} \approx 4 \cdot 10^3 \qquad (16)$$

$$Re_{\Delta x} = \frac{\rho v \Delta x}{\mu} \approx 4 \cdot 10^1 \qquad (17)$$

The axisymmetric geometrical model was discretized with a nonuniform mesh. The mesh distance was kept uniform in the upper part of the computational domain, containing the liquid and mushy regions, and was gradually sparsened in the z direction in the lower solid part of the domain. The domain has to be long enough in the z direction to ensure proper solution of the temperature field, since heat is conducted through the solid part of the billet. The domain length was 1.0 m in the case without species transport (**Figure 1**) and 0.8 m in the full macrosegregation case (**Figures 2-5**).

Table 1: Boundary conditions for mold and direct-chill zones [11,15]
Preglednica 1: Robni pogoji za področji kokile in neposrednega hlajenja s filmom hladila [11,15]

Position /m	h_{chill} / (W/m^{2}K)
$-0.00 > z > -0.12$	0
$-0.12 > z > -0.18$	$150\ g_s + 1500\ g_l$
$-0.18 > z > -0.19$	$150 + \frac{z[m]+0.18}{-0.19+0.18}(20000-150)$
$-0.19 > z > -0.23$	$20000 + \frac{z[m]+0.19}{-0.23+0.19}(10000-20000)$
$-0.23 > z$	10000

3 RESULTS AND DISCUSSION

Before proceeding to the full macrosegregation problem, the partial problem of coupled heat transfer and fluid flow was solved to approximately characterize the quality of the velocity-field solution. Since advection by liquid flow is the main mechanism of species transfer, a correct flow solution is important for a correct macrosegregation simulation. Because of the awareness of the presence of numerical errors and slow mesh convergence inherent of the first order scheme, which was used to ensure stability, a mesh convergence study was made. Some of the results are shown in **Figure 1**, where profiles of the vertical velocity component along the billet centerline are shown, as obtained in calculations on four different computational meshes, with the mesh spacing gradually decreasing by a factor of 2. It was found that even the solution on the densest mesh was not sufficiently close to the asymptotic convergence range, where convergence could be well characterized. However, due to a prohibitive increase in the computation time with mesh refinement, the mesh was not refined further.

The simulation of macrosegregation was made on a domain with reduced length $L = 0.80$ m, using a 136 × 252 finite-volume mesh. The mixture concentration field in the billet is shown in **Figure 4**. **Figure 3** shows the corresponding velocity and liquid-fraction fields.

In the case without species transport only thermal natural convection is present, and it causes a clockwise

Table 2: Thermo-physical properties of Al-4.5%Cu [11,15]
Preglednica 2: Snovne lastnosti zlitine Al-4.5%Cu [11,15]

Solid density	ρ_s	kg/m^3	2750
Liquid density	ρ_l	kg/m^3	2460
Solid specific heat	c_{ps}	J/kgK	958
Liquid specific heat	c_{ps}	J/kgK	1054
Solid thermal cond.	k_s	W/mK	180
Liquid thermal cond.	k_l	W/mK	95
Solid diffusivity	D_s	m^2/s	$5 \cdot 10^{-12}$
Liquid diffusivity	D_{sl}	m^2/s	$5 \cdot 10^{-9}$
Latent heat at eutectic	L_{eut}	J/kg	$3.90 \cdot 10^5$
Viscosity	μ	Pa s	$1.3 \cdot 10^{-3}$
Thermal expansion c.	β_T	K^{-1}	$1.17 \cdot 10^{-4}$
Solutal expansion c.	β_C		-0.73
Reference temperature	T_0	K	950
Reference concentration	C_0	–	0.045
Reference density	ρ_0	kg/m^3	2460
Permeability constant	K_0	–	$6.67 \cdot 10^{-11}$

circulation in the liquid sump. The flow velocity is large enough to cause a net upward flow (in terms of absolute velocity) in the billet center, while part of the flow deflects downwards in the center due to inertia. In the full problem (**Figures 2-5**) the flow is modified due to the influence of solutal buoyancy. As can be seen in **Figure 2**, the liquid is relatively quiescent at the bottom and in the center of the liquid sump, which appears to be caused by the counteracting effect of thermal buoyancy and the layering tendency of the heavy high-concentration liquid. Next to the liquidus front a complex flow structure consisting of small vortices forms. Five
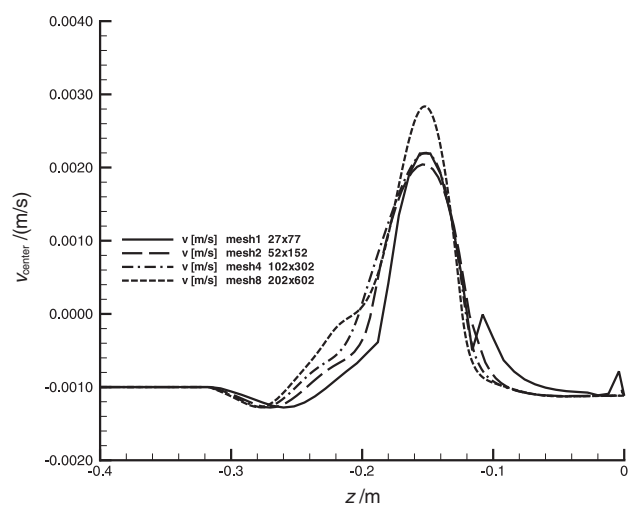
Figure 1: Vertical velocity component (v) profiles along the billet centerline obtained in the computations without species transport
Slika 1: Profili navpične komponente hitrosti (v) vzdolž središčnice droga, dobljeni pri izračunih brez upoštevanja transporta sestavin
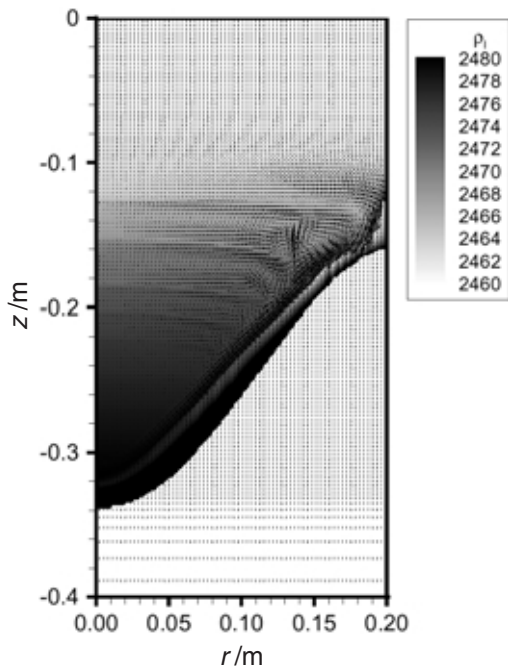
Figure 2: Liquid density (ρ_l) and absolute velocity (v) fields in the billet obtained in the full macrosegregation computation. The density field is shown only in the liquid and mushy zones ($f_l > 0$).

Slika 2: Polji gostote kapljevine (ρ_l) in absolutne hitrosti (v) v drogu, dobljeni pri izračunu makroizcejanja. Polje gostote je prikazano le v kapljevinastem in kašastem področju ($f_l > 0$).

vertically arranged flow cells can be identified, delimited by large density gradients. Each cell contains one or two vortices of thermosolutal origin. The whole flow
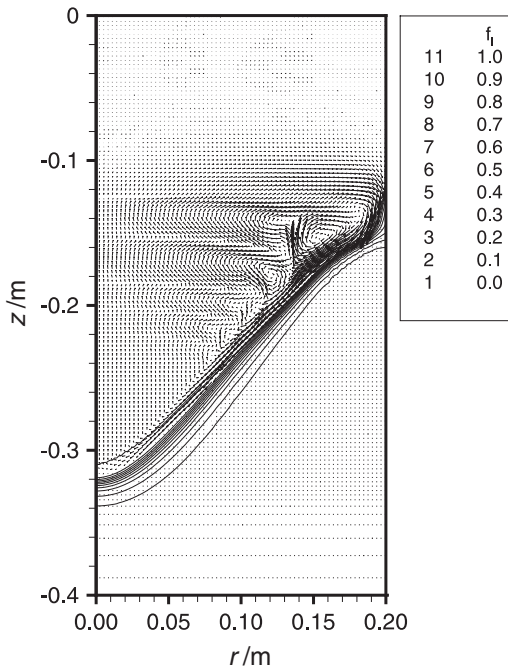
Figure 3: Relative velocity field (v-v_{cast}) and liquid fraction isopleths in the billet obtained in the full macrosegregation computation

Slika 3: Polje relativne hitrosti (v-v_{cast}) in linije konstantnega deleža kapljevinaste faze v drogu, dobljeno pri izračunu makroizcejanja
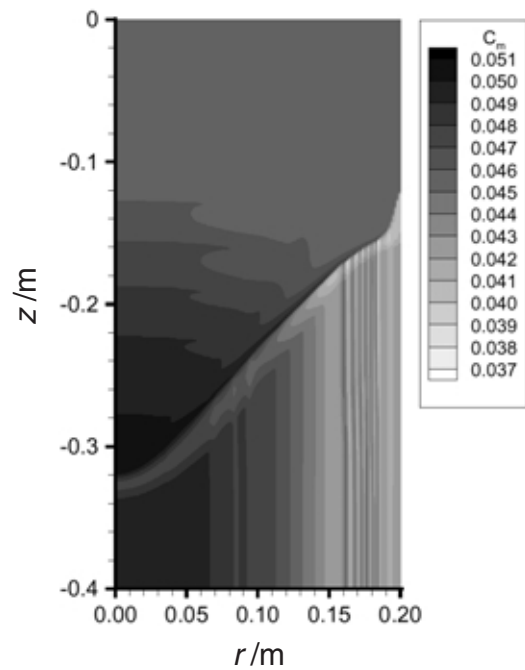
Figure 4: Mixture Cu concentration (C_m) field in the billet
Slika 4: Polje koncentracije Cu mešanice (C_m) v drogu

structure close to the liquidus front seems to be very complex and further studies will be necessary to determine and explain it more accurately.

In the solidification zone the liquid is enriched due to segregation of the solute ($C_l > C_m$; $C_s < C_m$). Since copper has a larger density than aluminum, a solutal downward flow of enriched liquid can be observed in the high-f_l portion of the mushy zone (along the liquidus front). This flow carries enriched liquid away from the top-subsurface part (top right in **Figure 4**) of the mushy zone, replacing it with lower-concentration liquid, which
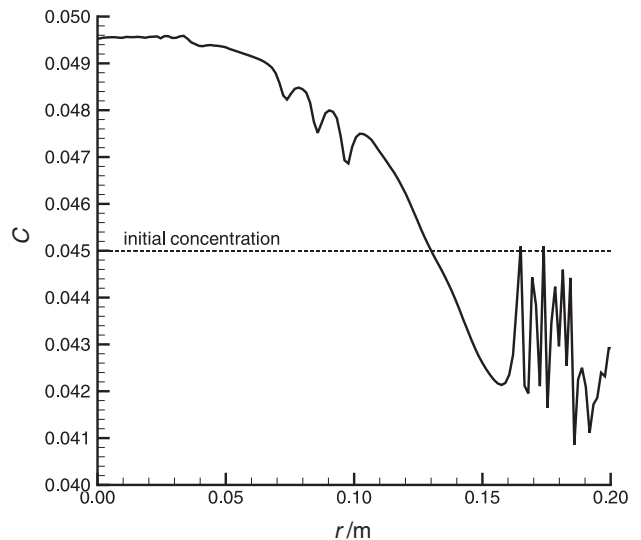
Figure 5: Radial Cu concentration profile in the solidified billet
Slika 5: Radialni profil koncentracije Cu v strjenem drogu

penetrates into the mush from the bulk liquid region. The heavy, enriched liquid flows down the slope of the mushy zone front, accumulating at the bottom of the sump. As the circulation, driven by thermal convection, carries some high concentration liquid out of the mushy zone into the bulk-liquid sump, smaller circulations, driven by strong solutal buoyancy can be observed. They are characterized by a rapid deflection back downward due to the strong effect of increased density. In the low-f_l regions of the mushy zone the permeability of the porous mush rapidly decreases. Therefore, the buoyancy and inertia do not influence the flow, and so the drag forces dominate. The flow is driven mostly by solidification shrinkage, as the liquid fills up the space left by the shrunken solidified metal. The liquid in the low-f_l mushy region is highly segregated (phase diagram), thus even small relative velocities can result in considerable net solute transport. This can be clearly seen along the whole mushy zone. The direction of the shrinkage-induced flow is parallel to the liquid fraction gradient. As the enriched liquid flows towards the solidus front it is replaced by the lower concentration liquid from regions of the mushy zone with higher f_l. The mushy zone thus appears as solute-depleted in terms of the mixture concentration. Flowing towards the solidus front, the enriched liquid accumulates at the front and the concentration rapidly increases in the direction normal to the f_l gradient. This is the mechanism causing typical positive subsurface segregation. Also, due to the predominance of shrinkage flow in the densely packed mushy zone, the segregation regions can already be identified before solidification is complete. There is no solute transport along the solidification front anymore.

The resulting macrosegregation profile, shown in **Figure 5**, does not properly predict the commonly observed distribution, characterized by a solute-depleted region in the billet center, adjoined by a positive segregation zone spreading in the outward radial direction, an adjacent thin negative segregation zone and another positive segregation layer at the surface. The reasons are believed to be deficiencies with the present model. They can be divided into numerical and physical modeling. Both significantly influence the macrosegregation prediction. The discrepancy in the centerline segregation is clearly a consequence of the simplified physical model, which lacks a description of the transport of low-concentration free-floating crystal grains, which are thought to sediment at the bottom of the sump and cause the common negative centerline segregation [1,4,15]. Instead, the present model logically predicts a settling of heavy copper-rich liquid at the sump bottom, which results in positive centerline segregation. The numerical deficiencies are related to use of upwinding in cases with large $Pe_{\Delta x}$ and $Re_{\Delta x}$ (Equations (16), (17)), where it causes considerable diffusion-like numerical discretization errors. While the presented macrosegregation model is at the beginning of its development, and was not expected to definitely explain the mechanism of macrosegregation in DC casting, the two separate problems that were identified, point out the relevant issues for further work. First, the numerical difficulties have to be elucidated and resolved. The verification can proceed through systematic convergence studies [17] and a comparison with solutions that use alternative methods [18]. Only after a satisfactory solution of the model equations is achieved, the physical model has to be extended. Presently, the effect of solute transport by free-floating crystal grains seems to be the most important physical mechanism for further study.

4 CONCLUSIONS

Simulations of macrosegregation in DC casting of a binary aluminum alloy were performed using a classical solidification model. An analysis of the computational results showed a rather complex interplay of predominantly advective species transport modes (double-diffusive convection and shrinkage flows) and has provided explanations for the predicted macrosegregation pattern. The predicted concentration profile is similar to those previously obtained in refs. [11,15]. While numerical problems regarding the solution of species transport are known from the literature and were recognized in macrosegregation results presented here, difficulties in obtaining a high-quality flow-field solution were shown on a reduced model (disregarding transport of species). Numerical and physical modeling issues for further research were identified, which are to bring us closer to understanding and a quantitative prediction of the macrosegregation formation in DC casting.

NOMENCLATURE

C	mass concentration of copper
C_0	reference concentration in buoyancy term
c_p	specific heat
D	mass diffusivity
f	phase mass fraction
g	phase volume fraction
$\vec{g}$	gravitational acceleration

h	specific enthalpy
h_{chill}	heat transfer coefficient at chill
k	thermal conductivity
K	permeability
k_{p}	binary equilibrium partition ratio
L	computational domain length
L_{eut}	latent heat of fusion at eutectic
m	mass
m_{L}	liquidus line slope
p	pressure
$Pe_{\Delta x}$	mesh Peclet number
r, z	cylindrical coordinates
$Re_{\Delta x}$	mesh Reynolds number
t	time
T	temperature
T_0	reference temperature in buoyancy term
T_{eut}	eutectic temperature
v	vertical velocity component
$\vec{v}$	velocity
V	volume
Δx	mesh distance
β_{T}	volumetric thermal expansion coefficient
β_{C}	volumetric solutal expansion coefficient
μ	dynamic viscosity
ρ	density
ρ_0	reference density in buoyancy term
l	liquid
m	mixture
s	solid
s	solidus
$*$	equilibrium conditions

5 REFERENCES

[1] H. Yu, D. A. Granger, Macrosegregation in aluminum alloy ingot cast by the semicontinuous direct chill (DC) method, Aluminum Alloys: Their Physical and Mechanical Properties, EMAS, UK, 1986, 17–29

[2] T. L. Finn, M. G. Chu, W. D. Bennon: The influence of mushy region microstructure on macrosegregation in direct chill cast aluminum-copper round ingots, Micro/Macro Scale Phenomena in Solidification, ASME, New York, 1992, 17–24

[3] C. J. Vreeman, M. J. M. Krane, F. P. Incropera, The effect of free-floating dendrites and convection on macrosegregation in direct chill cast aluminum alloys, part I: Model development, International Journal of Heat and Mass Transfer, 43(**2000**)5, 677–686

[4] C. J. Vreeman, M. J. M. Krane, J. D. Schloz, Direct chill casting of aluminum alloys: Modeling and experiments on industrial scale ingots, Journal of Heat Transfer ASME, 124(**2002**)10, 947–953

[5] S. C. Flood, L. Katgerman, V. R. Voller: The calculation of macro-segregation and heat and fluid flows in the DC casting of aluminum alloys, Modeling of Casting, Welding and Advanced Solidification Processes V, TMS, 1991, 683-690

[6] A. V. Reddy, C. Beckermann, Modeling of macrosegregation due to thermosolutal convection and contraction driven flow in direct chill continuous casting of an Al-Cu round ingot, Metallurgical and Materials Transactions B, 28B(**1997**)3, 479–489

[7] H. J. Thevik, A. Mo, T. Rusten, A mathematical model for surface segregation in aluminum direct chill casting, Metallurgical and Materials Transactions B, 30B(**1999**)1, 135–142

[8] C. J. Vreeman, F. P. Incropera, Numerical discretization of species equation source terms in binary mixture models of solidification and their impact on macrosegregation in semicontinuous, direct chill casting systems, Numerical Heat Transfer B, 36(**1999**)1, 1–14

[9] N. Ahmad, H. Combeau, J.-L. Desbiolles, T. Jalanti, G. Lesoult, J. Rappaz, M. Rappaz, C. Stomp, Numerical simulation of segregation: a comparison between finite volume method and finite element method predictions and a confrontation with experiments, Metallurgical and Materials Transactions A, 29A(**1998**)2, 617–630

[10] C. Beckermann, Modeling of macrosegregation: Applications and future needs, International Materials Reviews, 47(**2002**)5, 243–261

[11] B. C. H. Venneker, L. Katgerman, Modelling issues in macro-segregation predictions in direct chill castings, Journal of Light Metals, 2(**2002**)3, 149–159

[12] W. D. Bennon, F. P. Incropera, A continuum model for momentum, heat and species transport in binary solid-liquid phase change systems. I. model formulation, International Journal of Heat and Mass Transfer, 30(**1987**)10, 2161–2170

[13] H. Combeau, J.-M. Drezet, A. Mo, M. Rappaz, Modeling of micro-segregation in macrosegregation computations, Metallurgical and Materials Transactions A, 27A(**1996**)8, 2314–2327

[14] J. Mencinger, Polkontinuirno ulivanje aluminijevih zlitin: izračun časovnega razvoja temperaturnega in hitrostnega polja (in slovenian; Direct chill casting of aluminum alloys: Calculation of time evolution of temperature and velocity fields), Technical report, Politehnika Nova Gorica, 2002

[15] C. J. Vreeman, F. P. Incropera, The effect of free-floating dendrites and convection on macrosegregation in direct chill cast aluminum alloys, part II: Predictions for Al-Cu and Al-Mg alloys, International Journal of Heat and Mass Transfer, 43(**2000**)5, 687–704

[16] J. H. Ferziger, M. Perić, Computational Methods for Fluid Dynamics, Springer Verlag, 2nd edition, 1996

[17] P. J. Roache, Verification and Validation in Computational Science and Engineering, Hermosa publishers, Albuquerque, 1998

[18] B. Šarler, J. Mencinger, Solution of temperature field in DC cast aluminium alloy billet by the dual reciprocity boundary element method, International Journal of Numerical Methods for Heat and Fluid Flow 9(**1999**)3, 269–297